Reviewed Preprint
v1 • November 27, 2024
Not revised

Reviewed Preprint
v2 • February 17, 2026
Revised by authors

For correspondence:
james.marks@vanderbilt.edu
markus.hafner@nih.gov

* Department of Biochemistry, Vanderbilt University School of Medicine, Nashville, United States

** Department of Biological Anthropology, University of California, Los Angeles, Los Angeles, United States

Competing interests: No competing interests declared

Funding: See page 18

Reviewing editor: Daniel Arango, Northwestern University, United States

Determining the off-target activity of antibiotics and novel translation initiation sites in mitochondria

James Marks*, Emma Young, Markus Hafner**

RNA Molecular Biology Laboratory, National Institute for Arthritis and Musculoskeletal and Skin Diseases, NIH, Bethesda, United States

eLife Assessment

This **valuable** study presents findings on how prokaryotic antibiotics affect translation in mitochondrial ribosomes. Using mitoribosome profiling, the authors provide **solid** evidence that most tested antibiotics act similarly on bacterial and mitochondrial translation. Additionally, this work shows that alternative translation initiation events might exist in two specific mt-mRNAs (*MT-ND1* and *MT-ND5*). However, additional biochemical and structural experiments are needed to support these findings.

https://doi.org/10.7554/eLife.103699.2.sa3

Abstract

The 13 mtDNA-encoded proteins are synthesized using a dedicated translation system that is more similar to bacterial systems than the cytoplasmic system. Consequently, many bacterial protein synthesis inhibitors, used as antibiotics, exhibit mitochondrial toxicity as off-target effects. However, whether these antibiotics act through the same mechanisms in mitochondria as in bacteria remains unclear. To address this, we characterized the impact of a panel of bacterial translation initiation and elongation inhibitors on mitochondrial translation through mitoribosome profiling. We found that the mechanism of action for every antibiotic, except telithromycin, is the same in both bacteria and mitochondria. Additionally, mitoribosome profiling data showed that *MT-ND1* and *MT-ND5* have incorrectly annotated translation initiation sites and suggested the presence of several translation initiation sites on ncRNAs that produce mitoribosome footprints, as indicated by the detection of mitoribosome footprints at these locations. This work demonstrates how antibiotics can inhibit mitochondrial translation by mechanisms identically or very similar to those found in bacteria and the utility of mitoribosome profiling for annotating mitochondrial genes.

Introduction

Mitochondria contain their own genome, which canonically encodes thirteen proteins. These proteins are essential building blocks of complexes I, III, and IV of the electron transport chain, as well as ATP synthetase. They are synthesized at the mitochondrial matrix by a dedicated translation system that is conserved from the ancestral bacteria that evolved into the present-day organelles through an endosymbiotic event[1]. As a result, mitochondrial translation is wholly distinct from cytoplasmic translation and utilizes its own mitochondrial ribosomes (mitoribosomes), tRNAs, and translation factors. The RNA components of the machinery are mitochondrially encoded, while its protein components are encoded in the nucleus, translated by the cytoplasmic ribosome, and subsequently imported into the mitochondria[2].

Chronic impairment of mitochondrial translation, most commonly through mutations in translation factors, results in disrupted mitochondrial function and causes diseases such as MERRF (Myoclonic Epilepsy with Ragged-Red Fibers)[3], MELAS (Mitochondrial Encephalopathy,

Lactic Acidosis, and Stroke-like episodes)[4], and maternally inherited deafness[5,6]. Furthermore, acute inhibition of mitochondrial translation caused by the off-target action of antibiotics targeting the bacterial ribosome can also cause mitochondrial toxicity[7–11]. This toxicity can manifest as lactic acidosis, ototoxicity[12], nephrotoxicity[13], and peripheral neuropathy[14], depending on the specific antibiotic and the genetic background of the recipient[15]. While the United States has worked to regulate antibiotics with severe side effects, they remain a global issue. For example, chloramphenicol, whose use is discontinued in the United States, causes fatal aplastic anemia at a rate of 1 in 60,000[7] but remains widely prescribed in low-income countries due to its low production cost[16,17]. Surveys suggest that approximately 14.3 doses of antibiotics are administered per 1,000 people every day worldwide[18]. The toxic effects of antibiotics can be exacerbated when taken without medical supervision. In addition, safety concerns surrounding drugs like chloramphenicol and telithromycin, which are linked to liver failure[19], limit our pool of available antibiotics in the face of a rise in multidrug-resistant bacteria. Studying the off-target effects of these drugs can guide the development of safer therapies.

Multiple classes of antibiotics inhibit bacterial translation by binding functionally important sites on the ribosome and disrupting a specific process in translation, resulting in arrested translation on mRNAs at sites characteristic of the mechanism of inhibition[20,21]. In some instances, this relationship is straightforward. For example, the pleuromutilin antibiotic retapamulin binds to the peptidyl-transferase center (PTC) of the bacterial ribosome and impedes translation initiation by interfering with the positioning of initiator tRNA[22], resulting in bacterial ribosomes accumulating at start codons[23]. Inhibition by other antibiotics is more complicated, only disrupting translation when specific sequences are being translated, called context-dependent translation arrest. This is exemplified by chloramphenicol, which simultaneously interacts with the nascent peptide and the peptidyl-transferase center at its binding site and disrupts accommodation of aminoacyl-tRNA, thereby acting as an elongation inhibitor[24]. Due to chloramphenicol's interaction with the nascent peptide, it selectively causes ribosomes to arrest translation when an alanine, serine, or threonine is in the –1 (penultimate) position of the nascent peptide[25]. Additionally, chloramphenicol does not interfere with the accommodation of glycine due to its minimal size. The mechanisms of these and other antibiotics in bacteria have been determined by ribosome profiling and structural studies. As well, structural studies have demonstrated the binding characteristics of antibiotics on the mitochondrial ribosome[11,26,27]. However, it remains unclear whether chloramphenicol or other antibiotics inhibit mitochondrial translation by identical mechanisms.

To determine the sites of translation arrest, we utilized mitoribosome profiling in HEK293 cells treated with a diverse panel of antibiotics[19,28,29]. Ribosome profiling allows for the mapping of translating ribosomes with codon-level accuracy by identifying mRNA sequences occupied by translating ribosomes. To do this, RNase treatment degrades mRNA unprotected by the ribosome to generate ribosome-protected fragments (RPFs). Because cytoplasmic ribosomes significantly outnumber mitoribosomes, mitoribosomes containing the mitochondrial RPFs (MRPFs) are isolated through sucrose gradient fractionation, where the cytoplasmic ribosome and mitoribosome sediment in the 80S and 55S fractions, respectively (Figure 1A). RPFs are isolated and quantified by next-generation sequencing. Increases in MRPFs reveal the specific codons and sequence contexts prevalent at sites at which mitochondrial translation arrests due to antibiotic treatment.

Understanding the mechanisms of translation inhibitors in mitochondria can guide the development of therapeutics that are more selective to the bacterial ribosome and lay the groundwork for determining how these therapeutics disrupt mitochondrial function. In this study, we utilized mitoribosome profiling in the presence of the bacterial protein synthesis inhibitors retapamulin, tiamulin, josamycin, erythromycin, chloramphenicol, and linezolid to determine their mechanism of action. We found that the mechanism of mitochondrial inhibition is the same as bacterial inhibition for all inhibitors except telithromycin. While telithromycin selectively arrests bacterial ribosomes when either arginine (R) or lysine (K) is in the −1 position of the nascent chain and A-site, called an R/K-X-R/K motif[30], it instead arrests mitochondrial translation at an R/K/A-X-K motif, suggesting an underlying difference in the mechanism of the two systems.

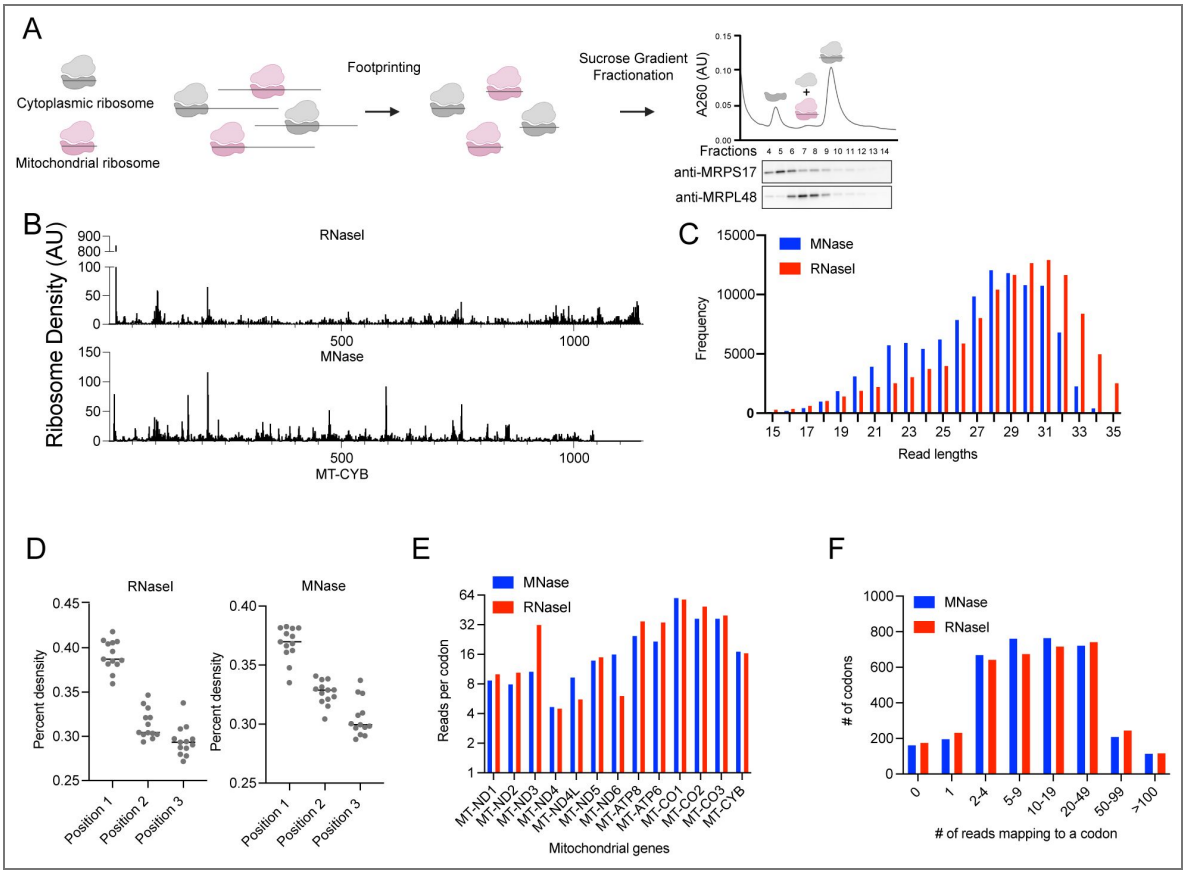

Figure 1. **Mitoribosome profiling captures elongating ribosomes.**

(A) Schematic representation of mitoribosome footprinting and separation from cytoplasmic ribosomes by differential centrifugation. (B) Coverage of MRPFs on *MT-CYB* from mitoribosome profiling generated by either RNase I or MNase footprinting. (C) Distribution of read lengths of MRPFs mapping to the mitochondrial genome. (D) Read phasing analysis of MRPFs, where the 5′ ends of reads are grouped by their subcodon position. Each dot represents an individual mitochondrial gene. (E) Average coverage of mitochondrial genes, calculated by dividing the total number of reads mapping to an ORF and dividing by the length of the ORF. (F) Distribution of mitochondrial codons grouped by the number of mitoribosome P-sites assigned to them.

Additionally, nucleotide-level precision of mitoribosome profiling also allowed us to precisely annotate the mitochondrial gene structure. We found that *MT-ND1* and *MT-ND5* genes use alternative translation initiation sites and identified a putative open reading frame on the *MT-RNR1* gene. This work demonstrates that mitoribosome profiling is an effective tool to study the fundamentals of mitochondrial translation and the mechanisms of translation impairment affecting human health.

Results

RNase I generates highly phased mitoribosome footprints

To optimize the mitoribosome profiling method, we tested two different RNases typically used for ribosome footprinting, RNase I and MNase, followed by the isolation of the 55S mitoribosome by sucrose gradient fractionation. We mapped the sequence reads to the mitochondrial genome and its thirteen open reading frames (ORFs). For each mapped sequence read, we inferred the position of the ribosomal P-site using a 13-nucleotide (nt) offset from the 5' end, determined by the analysis of footprint distribution surrounding the initiation sites of *MT-ND4*, *MT-ND6*, and the newly reported *MT-ND5-dORF*. We observed coverage across mitochondrial ORFs, suggesting we captured translating mitoribosomes (Figure 1B). Furthermore, analysis of MRPF lengths revealed a distinct difference between the RNase I and MNase-digested footprint. While both libraries are enriched for reads ~30 nt in length, MNase footprints showed a bimodal distribution, with a clear secondary peak at ~22 nts (Figure 1C), which may indicate that MNase-treatment may have captured two distinct conformations of the ribosome. To determine the quality of the ribosome profiling data, we calculated read phasing, which occurs when a nuclease creates uniform MRPFs and the resulting ends of the MRPFs reflect the 3-nt periodicity of elongating ribosomes. While both datasets do show clear phasing, the read phasing is more biased toward position 1 of the codon in the RNase I-treated sample, indicating slightly more consistent digestion (Figure 1D, Table S1). Nevertheless, we observed similar levels of footprint abundance per gene, with the only notable exceptions being that RNase I-digested footprints were enriched on *MT-ND3* and depleted on *MT-ND4L* and *MT-ND6* (Figure 1E). While the cause of the difference is unclear, we did not expect it to interfere when comparing an antibiotic-treated sample to a control. Read coverage also appeared similar across the two methods, with 85%-87% codons having between 2 and 50 reads mapping to them (Figure 1F). Overall, these results indicated that both MNase and RNase I digestion capture mitoribosome footprints with only minor differences. Considering the improved read phasing, we selected RNase I for our subsequent mitoribosome profiling experiments.

Retapamulin, tiamulin, and josamycin inhibit translation initiation

First, we examined the impact of three antibiotics – retapamulin, josamycin, and tiamulin – on translation initiation or mitochondrial translation. Retapamulin and tiamulin are members of the pleuromutilin class of antibiotics. They work by binding to the peptidyl transferase center (PTC) of the bacterial ribosome and disrupting initiator tRNA and A site tRNA positioning (Figure 2A, left)[22,23,31–33]. Josamycin is a macrolide antibiotic that binds in the nascent peptide exit tunnel near the PTC and arrests bacterial ribosomes at initiation by interfering with A-site tRNA positioning (Figure 2A, right)[34]. We sought to understand whether these antibiotics also target translation initiation in mitochondria. To this end, we treated HEK293 cells with high concentrations of these antibiotics (100 µg/ml of tiamulin and josamycin, 10 µg/mL of retapamulin) for 30 minutes, performed mitoribosome profiling, and compared the treated experiments to a DMSO-treated control.

We mapped MRPFs to the 13 mitochondrial genes. On *MT-CYB* and all other genes, we observed that after treatment with antibiotics, reads accumulated at the 5' end of the transcript and MRPFs across the rest of the coding region were lost or decreased (Figures 2B, S1). We quantified the percentage of MRPFs mapping at the 5' end relative to the total ORF, excluding polycistronic mRNAs. Treatment with translation initiation inhibitors increased the percentage of those reads

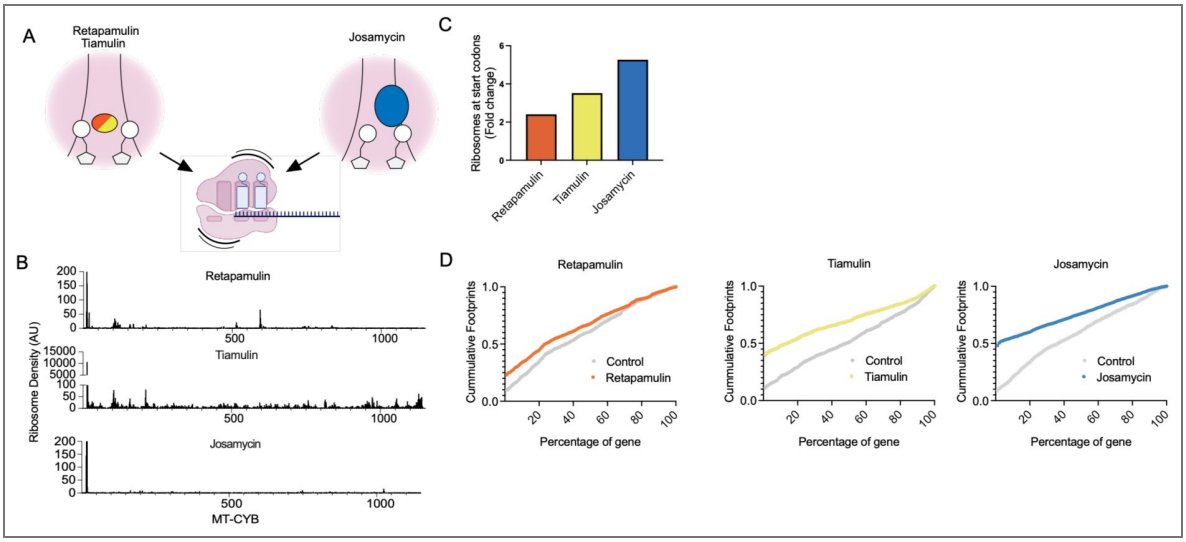

Figure 2. Inhibition of translation initiation in mitochondria.

(A) (Left) Schematic representation of retapamulin (orange) or tiamulin (yellow) binding to the PTC and disrupting the first round of elongation. (Right) Josamycin (blue) disrupts accommodation of the first aminoacyl-tRNA. All three inhibit initiation in bacteria. (B) MRPF coverage of *MT-CYB* treated with either retapamulin, tiamulin (note y-axis is segmented), or josamycin. (C) Average fold change increase in the percentage of reads that map to the 5′ of mitochondrial transcripts. (D) Cumulative distribution of ribosome density normalized across all mitochondrial ORFs.

from 2.4 to 5.2-fold relative to the DMSO-treated cells (Figure 2C). Additionally, we quantified the cumulative footprint abundance moving from the start to the stop codon (Figure 2D). While ribosome footprints are generally evenly spread across the open reading frame in the DMSO control, MRPFs from cells treated with the initiation inhibitors showed a sharp increase in the percentage of reads found at the 5' end. Together, these results indicate that retapamulin, tiamulin, and josamycin inhibit mitochondrial translation initiation, likely by the same mechanism as in prokaryotes.

Chloramphenicol, linezolid, and telithromycin arrest mitochondrial translation in a context-dependent manner

Chloramphenicol, linezolid, and telithromycin selectively inhibit bacterial translation when ribosomes are translating specific sequences, in a process called context-dependent translation arrest[25,30]. Linezolid, like chloramphenicol, induces context-dependent arrest when alanine, serine, or threonine is at the penultimate position of the nascent peptide (Figure 3A, left). Unlike chloramphenicol and linezolid, telithromycin binds in the nascent peptide exit tunnel near the PTC and adjacent to the nascent peptide[35]. During elongation, telithromycin causes ribosomes to arrest translation at an R/K-X-R/K motif, when the identity of both the penultimate position of the nascent peptide and the incoming aminoacyl-moiety is either arginine or lysine (Figure 3A, right). We carried out mitoribosome profiling on HEK293 cells treated with either antibiotic to understand whether these context-dependent translation inhibitors arrest mitoribosomes in the same manner as they arrest bacterial ribosomes. Unlike the cells treated with initiation inhibitors, cells treated with chloramphenicol or linezolid carried ribosome density throughout the entirety of the ORF, suggesting that, as expected, they were not acting as inhibitors of initiation (Figures 3B, S1). Cells treated with telithromycin did show a slight increase in MRPFs abundance at the 5' end of *MT-CYB*. However, across all genes, the levels of MRPFs at the 5' end were not near the levels seen when using the initiation inhibitor retapamulin and were more similar to chloramphenicol, linezolid, and the DMSO control (Figure 3C). The cumulative distribution of MRPFs suggested that ribosome density was biased towards the 5' end of the gene for chloramphenicol and telithromycin, but not significantly for linezolid (Figure 3D). These results suggest that these three antibiotics are not acting as initiation inhibitors and that linezolid and telithromycin redistribute MRPFs to the 5' end of the ORF.

Next, we determined whether this observed redistribution of elongating ribosomes was dependent on the context of the sequence being translated. We calculated the average change of MRPFs depending on the identity of the amino acid at either the −1, P-site, or A-site positions. For both chloramphenicol and linezolid, we observed a specific increase in ribosome footprints when mitoribosomes encountered codons for alanine, serine, or threonine in the −1 position, with a 2-, 2.2-, and 1.3-fold change for chloramphenicol and a 2.3-, 1.4-, and 1.6-fold change for linezolid, respectively (Figure 3E). Additionally, we also observed context-dependent translation arrest induced by telithromycin. Unlike the R/K-X-R/K motif observed in bacteria, we found that telithromycin caused mitoribosomes to arrest at sites with a lysine positioned in the A-site, with an average 2.5-fold increase in MRPFs around those sites, and that neither residue was enriched in the −1 position. Due to the limited size of the mitochondrial genome, there are only nine instances of the R/K-X-R/K motif; nevertheless, when we observed the positions with the greatest fold change, 3 of the top 4 contained the motif with lysine in the A-site (Figure 3F), suggesting that the motif was at least partially recapitulated. To specifically look for the motif, we calculated the average fold change when we fixed arginine or lysine in the A-site and varied the identity of the −1 amino acid (Figure 3G). We found that when lysine was in the A-site while either arginine, lysine, or alanine was in the −1 position, there was strong arrest (> 5-fold change). However, when arginine was in the A-site, we did not observe a strong stalling event with any −1 position residue. Therefore, in mitochondria, telithromycin induces stalling at R/K/A-X-K motifs. This motif appears in only 6 of the 13 mitochondrially encoded genes, indicating that mitochondrial protein synthesis is unequally inhibited (Figure S2A, B). We concluded that the mechanism underlying context-dependent translation arrest for telithromycin is different in mitochondria compared to bacteria.

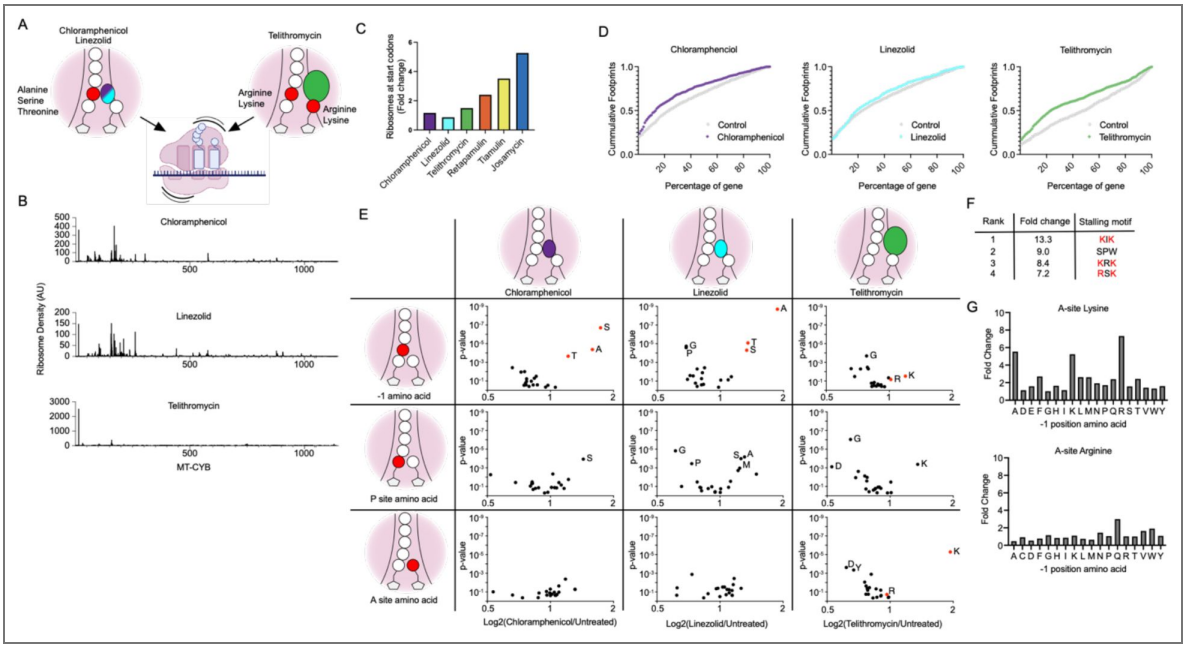

Figure 3. Context-dependent translation arrest by elongation inhibitors.

(A) Schematic representation of chloramphenicol (purple), linezolid (cyan), and telithromycin (green) inducing context-dependent translation arrest. (B) MRPF coverage of *MT-CYB* from cells treated with either chloramphenicol, linezolid, or telithromycin. (C) Average fold change increase in the percentage of reads that map to the 5′ of mitochondrial transcripts. (D) Cumulative distribution of ribosome density normalized across all mitochondrial ORFs. (E) Volcano plots of changes in MRPF fold change from cells treated with translation inhibitors. Each dot is the mean $\log_2$-fold change grouped by the identity of the −1 amino acid (top), P-site amino acid (middle), or A-site amino acid (right). (F) The top 4 strongest stalling sites induced by telithromycin treatment. Red amino acids indicate a classical R/K-X-R/K stalling motif. (G) Fold change in ribosome density, calculated as $2^{\text{mean}(\log2(\text{Telithromycin/Control}))}$. Bars differ in the identity of the P-site amino acid and contain either a lysine in the A-site (top) or arginine (bottom).

Translation initiation on *MT-ND1 and MT-ND5* occurs at an alternative start codon

During the process of assigning the P-site positions of MRPFs, we observed that no ribosomes were assigned in the first 13 nucleotides of the 5' end of the transcript. This is not surprising, considering that mitochondrial transcripts often have no or very short 5' untranslated regions - typically less than 4 nts long - and we applied a 13-nt offset from the 5' end of MRPFs. It reasons that as mitoribosomes begin translation on a leaderless mRNA, the 5' end of the resulting MRPF would have a full-length region 3' of the P-site and no sequence 5' of the P-site. As a ribosome moves down the transcript, the 5' end of the MRPF would increase until it is accessible for digestion, at which point it would generate 31 nt-long MRPFs (Figure 4A). As accurate mapping of mitoribosomes at initiation could be a useful tool to understand mitochondrial translation, we attempted to map the location of initiating mitoribosomes at the 5' end using footprint length, rather than the 5' offset. Because mitoribosome profiling with MNase generated a population of ribosomes with short MRPFs, we hypothesized that these footprints could be indicative of capturing initiating ribosomes (Figure 1C). We plotted the distribution of MRPFs from 20 to 34 nts in length that mapped to the 5' end of the 11 leaderless or short leader ORFs and compared them to reads mapping to the whole ORF. We observed that MRPFs 22-23 nts in length were 6-fold more abundant and MRPFs >28 nts in length were depleted compared to the whole ORF (Figure 4B). As mitochondrial ORFs vary in the length of their 5' UTR and we expect most ribosomes to be positioned at the start codon, we tested whether leaderless ORFs were enriched in shorter reads compared to ORFs preceded by a short leader. Leaderless ORFs, such as *MT-CO2*, *MT-CO3*, and *MT-ND4L*, contained MRPFs mainly 20-23 nucleotides in length at the 5' end (Figure 4C, top). *MT-ATP8*, which contains a start codon beginning at the third nt, contained footprints that were 22-24 nt long, and *MT-CO1*, with a start codon at the fourth nt, contained MRPFs 23-24 nt long (Figure 4C, middle). Not only did we observe longer MRPFs in short leader ORFs, but the size of the MRPFs also appeared proportional to the location of the start codon. Together, these results indicate that the size of the footprint is directly related to the start codon position at the 5' end of mitochondrial mRNAs.

Two genes, *MT-ND*1 and *MT-ND5*, deviated from this trend. The annotated start site for *MT-ND5* is a leaderless AUA codon (a start codon in mitochondria), but we observed few 20-22 nt MRPFs (Figure 4C, bottom). Similarly, the annotated start site for *MT-ND1* is also an AUA codon that begins at the third nt, and it is depleted in reads for MRPFs that are smaller than 25 nts. Instead, MRPFs derived from the 5' end of both genes are enriched in longer reads: 27 nts-long for *MT-ND5* and 28-29 nts-long for *MT-ND1*. Curiously, the third codon for both genes is an in-frame AUG, and the read lengths proportionally correspond to mitoribosomes positioned at these codons, suggesting mitoribosomes initiate translation at these sites. MRPFs generated from cells treated with initiation inhibitors and footprinted by MNase yield similarly sized reads at the 5' end of *MT-ND1* and *MT-ND5* (Figure S3). Using protein mass spectrometry, we tested whether peptides matching the N-terminus of these proteins would correspond to initiation at the canonical start codons or alternative start codons. We identified a peptide that mapped to the N-terminal region of MT-ND1 but lacked the first two amino acids, accordant with translation initiating from the alternative start codon (Figure 4D). While we did not identify N-terminal peptides mapping to MT-ND5 from our mass spectrometry data, the protein mass spectrometry database MassIVE[34] covered the N-terminal region of MT-ND5 (Figure 4E). Consistent with our mitoribosome profiling data, the majority of N-terminal fragments did not include the amino acids from the annotated start or second codon but began with methionine at codon 3. We also observed that MRPFs on *MT-ND6*, which initiates at the first of two AUG codons immediately at the 5' end, correlated to ribosomes positioned at both AUG codons, indicating that this gene may initiate translation from the second AUG codon as well. However, we did not observe any peptides mapping to the N-terminus of *MT-ND6*. Together, these data show that *MT-ND1* and *MT-ND5* may not initiate from their canonical AUA codons but may use alternative in-frame AUG codons.

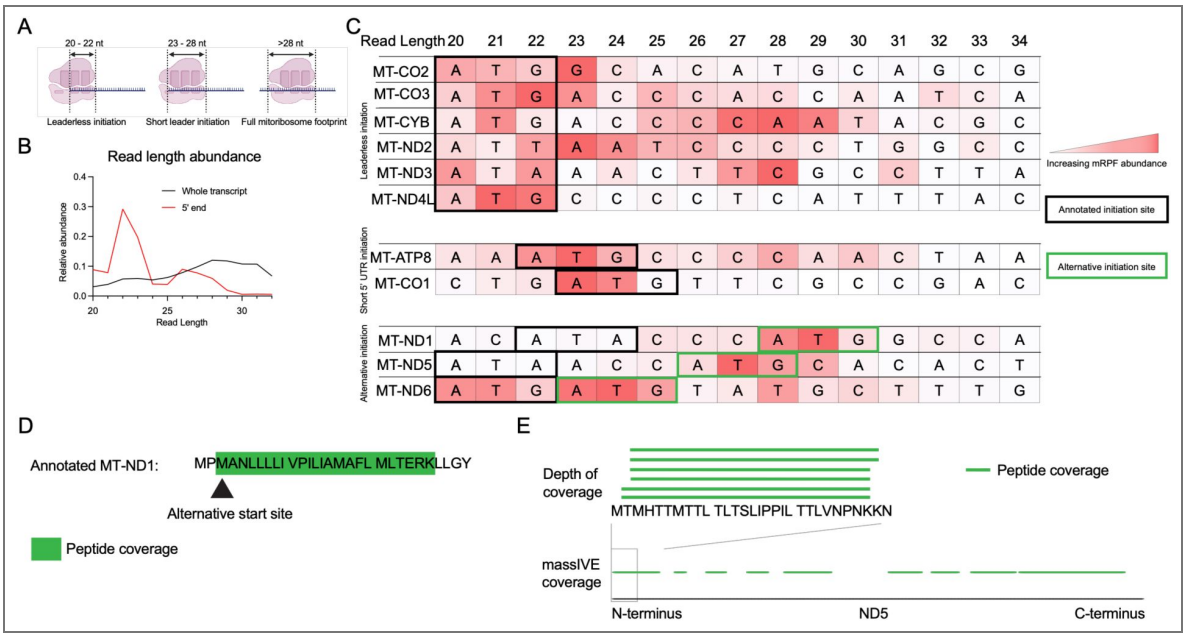

Figure 4. MRPF sizes indicate use of alternative initiation sites.

(A) Schematic representation of changing MRPF sizes as a function of the mitoribosome's position near the 3' end of mRNAs. (B) Read length measurement of reads mapping to the 5' ends of mitochondrial transcripts (red) compared to the entire ORF (black). (C) Read lengths of MRPFs mapping to the 5' ends of mitochondrial transcripts. Each row contains the nucleotide sequence of each transcript starting from the 5' end. The coloring of the box is proportional abundance of MRPFs with read lengths from 20-34 nts. Nucleotide sequence and read abundance are overlayed to compare the abundance of reads to potential ribosome start sites. Transcripts are grouped by being leaderless, having a leader, or having a potential alternative start site. Black boxes indicate annotated start codons and green boxes indicate alternative initiation sites. (D) Visual representation of the peptide coverage (green bars or highlights) from mass spectrometry data covering the N-terminus of *MT-ND1* or (E) *MT-ND5*.

Additionally, our findings indicate that the mapping of mitochondrial translation initiation events by size, rather than 5' offset, is an accurate strategy when used in conjunction with MNase footprinting.

Mitoribosome profiling may reveal novel translation events

During our analysis of 5' end mapping, we did not remove reads mapping to non-coding RNAs (ncRNAs) before mapping to the mitochondrial genome and performing P-site assignment. Consequently, we observed that some tRNAs and rRNAs had an abundance of reads mapping to 13 nts away from their 5' ends, similarly to what we observe on mRNAs for translation initiation. In addition, some of these ncRNAs contained a potential start codon near the 5' end. These reads could either be products of random digestion of the abundant background of ncRNAs or be genuine MRPFs. We hypothesized that if these reads were the result of mitoribosomes initiating or attempting to initiate translation at the 5' end of the ncRNAs, then we could use the same analysis of read length distribution at 5' ends of mRNAs we performed above and determine of the sizes correlated to an AUG, AUU, GUG, or UUG as potential start codons. While GUG and UUG are not used in canonical mitochondrial initiation, they were included in the search because noncanonical initiation has been observed at GUG[36], and both are frequently utilized in bacterial initiation. We identified sites on four tRNAs that contained MRPFs with a size that correlated to either AUG or UUG codons (Figure 5A). The predicted ORFs and thus resulting potential translation events varied widely. On *MT-TF*, the start codon is followed by an immediate stop codon. The ORF on *MT-TI* is three codons long and terminates with the non-canonical mitochondrial termination codon AGA. On *MT-TY, a* 7-codon ORF is terminated by a UAA codon. *MT-TS1* contains the largest open reading frame identified on tRNAs, at 20 codons, and it terminates with the U AGA sequence, as used in *MT-CO1*[37]. Additionally, we identified a putative start site at the 5' end of *MT-RNR1* (Figure 5A), and mitoribosome profiling of cells treated with initiation inhibitors and digested with MNase shows similar footprint sizes (Figure S3). However, this site did not occur at a canonical AUG or AUU codon, but instead at a UUG codon. This putative start codon is followed by a 58-codon ORF and terminates at a UAG stop codon.

To determine whether translation elongation occurs at these putative ORFs, we determined the read phasing characteristic for MRPFs derived from translating ribosomes at these ORFs. However, the sites on *MT-TF*, *MT-TI*, and *MT-TY* are short and close to the 5' end, hindering phasing analysis and thus do not allow us to conclude whether our sequence reads are indicative of translation. While the ORF on *MT-TS1* is longer, MRPF density was low, and we did not observe read phasing and thus it is likely not translated (not shown). The reads mapping to the ORF on *MT-RNR1* had a phasing profile similar to those mapping to the 13 canonical mitochondrial genes (Figure 5B). In contrast, reads mapping to the remainder of *MT-RNR1* or mapping to the region of *MT*-RNR2 that codes for the putative mitochondrial micropeptide Humanin show no or conflicting read phasing. When compared to the amino acid composition of the mitochondrially-encoded proteome, the amino acid composition of the resulting peptide shows a stronger positive correlation (R^2=0.534) (Figure 5C) to the remaining non-coding portion of *MT-RNR1* (R^2=0.241) (Figure 5D). Although mitoribosome profiling suggests that this putative ORF is translated, we did not detect any corresponding peptides in the protein mass spectrometry of isolated mitochondria. Nevertheless, our mass spectrometry dataset, or the MASSIVE database, does not cover many regions of the mitochondrial proteome, and thus, the absence of a spectrum is not necessarily evidence that the peptide is not translated. The read phasing analysis suggests this region of *MT-RNR1* is translated and could encode a 15th mitochondrial protein. Overall, this data shows that our mitoribosome profiling can be used as a tool to study non-canonical translation events resulting from ncRNAs.

Discussion

In this work, we sought to understand the mechanisms of bacterial protein synthesis inhibitors on their primary off-target, the mitoribosome. We found that inhibitors of bacterial translation initiation, retapamulin, tiamulin, and josamycin, also act as initiation inhibitors in mitochondria.

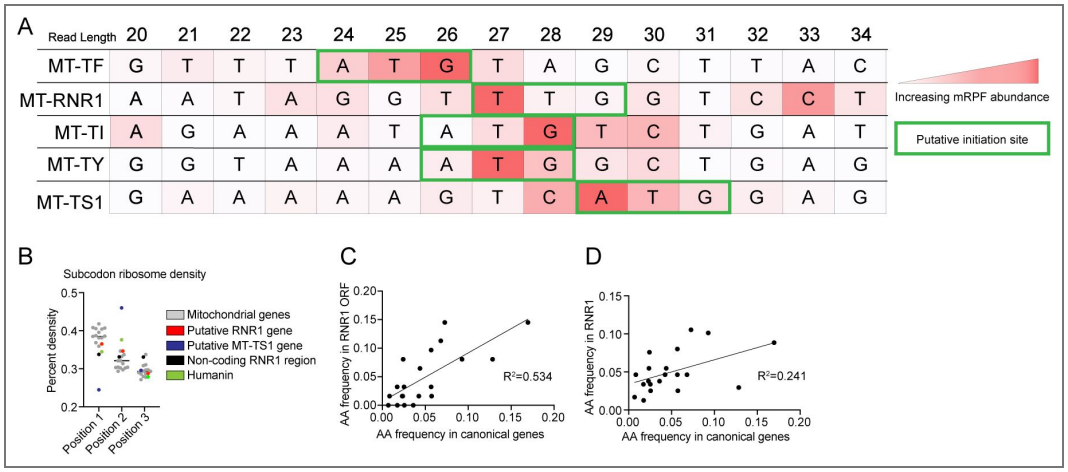

Figure 5. MRPFs on ncRNAs indicate potential novel ORFs

(A) Read lengths of MRPFs mapping to the 5′ end of ncRNAs. Each row contains the nucleotide sequence beginning from the 5′ end of listed ncRNAs. The coloring of the box is proportional the abundance of MRPFs with read lengths 20-34 nts. The nucleotide sequence and read MRPF abundance are overlayed to identify potential new start sites. Putative start sites are indicated by green boxes. (B) Read phasing analysis of all canonical ORFs (grey), a mutative ORF located on *MT-RNR1*, the non-coding region of *MT-RNR1*, and Humanin. (C) A correlation plot comparing the frequence of amino acid usage in canonical ORFs compared to the putative ORF on *MT-RNR1* or (D) the non-coding region of *MT-RNR1*.

Likewise, chloramphenicol and linezolid selectively inhibit elongation when the mitoribosome carries either an alanine, serine, or threonine in the penultimate position of the nascent peptide, matching their mechanism in bacteria. In contrast, the context-dependence of telithromycin differed when arresting mitoribosomes, wherein it preferentially arrested translation at the R/K/A-X-K motif.

Context-dependent translation arrest by chloramphenicol and linezolid suggests similarities between the binding of the bacterial ribosome and the mitoribosome. Structural and biochemical studies have demonstrated that binding of chloramphenicol and linezolid is stabilized by alanine, serine, or threonine in the penultimate position of nascent peptide[38,39]. Our findings suggest a similar or identical interaction is occurring in the mitoribosome. In contrast, these inhibitors are unable to inhibit peptide bond formation in bacteria when glycine is positioned in the A-site, due to the minimal size of the side chain, allowing the inhibitor and the aminoacyl-moiety to coexist in the PTC. We did not observe a lack of mitoribosome translation arrest when glycine was positioned in the A-site. This may have technical reasons, e.g., it may be caused by an insufficient depth in sequencing or indicate that the relatively small mitochondrial genome limits the variety of stalling and non-stalling events we can observe. But more likely it shows that chloramphenicol and linezolid are capable of arresting translation when glycine is in the A-site. Recently, mitoribosome profiling analysis showed that chloramphenicol added during lysis did not induce context-dependent translation arrest[40]. This suggests that during lysis, there is insufficient mitochondrial translation to induce a redistribution of mitoribosomes rather than an inability of the chloramphenicol to induce context-dependent arrest.

During the preparation of this manuscript, two other groups studied the effect of translation inhibitors on mitochondrial translation. One group's mitoribosome profiling in the presence of chloramphenicol and linezolid agreed with our observed context-dependent translation arrest[41]. The structure of linezolid in the mitochondrial peptidyl-transferase center also suggested some nuanced differences in binding between the bacterial and the mitochondrial ribosome. Another group carried out mitoribosome profiling in the presence of retapamulin[40]. However, they observed additional ribosome density throughout the coding region and potentially some associated with putative start codons. This differs significantly from our observed accumulation at only annotated start sites and may be due to differences in mitoribosome profiling methods. Future work may reveal how each strategy contributes to our understanding of mitochondrial translation.

Inhibition of mitochondrial translation through either small molecules or mutations localized in mitochondrial translation factors can induce a wide range of pathologies[42–44]. However, it is unclear how or whether the relationships between the mechanism of translation inhibition relate to the resulting disease. Recently, the proteins mtRF-R and MTRES1 were shown to act as quality control factors, rescuing stalled mitoribosomes by removing the nascent peptide and peptidyl-tRNA[45]. In addition, treatment with antibiotics can reduce the presence of polyamines in the mitoribosome, potentially reducing translation[46]. As the mitoribosome can arrest translation through a variety of mechanisms and small molecules, it remains unclear whether these factors can rescue all stalled mitoribosomes or decrease the translation rate to reduce the total amount of translation arrest. Further work to dissect the relationship between mechanisms of inhibition, activation of rescue factors, and stress response can complement our understanding of pathologies resulting from mitoribosomopathies and antibiotic treatment.

In this study, we also reported that the translation start codon of two mitochondrial genes, *MT-ND1* and *MT-ND5*, does not use the annotated AUA codon, but instead begins translation from a nearby in-frame AUG codon. Others have noted that haplogroups L1b and F2 contain a single nucleotide polymorphism at either position T3308C or T12338C, respectively, which disrupts the annotated AUA start codons of *MT-ND1* and *MT-ND5* yet does not result in any discernible pathogenicity[47–49]. The authors noted that the same AUG codons we identified as start codons could be used in lieu of the canonical AUA start codons. Because we observe MRPF lengths primarily correlating with the AUG codons, we suggest that these downstream start codons are the primary start site for these genes, though this does not preclude the use of both sites. Given the

limited examples of translation initiation sites inherent to the mitochondrial genome, the reannotation of 2 sites is a significant revision and can guide future work to understand how start codon selection occurs in mitochondria.

Recently, mitoribosome profiling was used to identify an open reading frame in region immediately 3' of the gene *MT-ND5*, which we confirmed observing in our profiling experiments[50]. However, this uses an internal initiation mechanism for polycistronic genes, similar to *MT-ND4* and *MT-ATP6*. Until now, accurate mapping of mitochondrial translation events at the 5' ends of transcripts has been unavailable. We identified MRPFs that map to putative start codons occurring on mitochondrial MT-tRNAs and *MT-RNR1*, based on the size of the reads occurring at the 5' end of the RNA and their relationship to a start codon localized in the sequence. The site of *MT-RNR1* was further supported by analysis of the resulting ORF, suggesting translation initiation and elongation occurs. Curiously, $tRNA^{Tyr}$, encoded by *MT-TY*, is polyadenylated during processing, which may be related to our identification of a ribosome binding event on this tRNA[51]. Due to both the short ORFs, minimal read coverage, and lack of a detectable peptide we could not determine if translation elongation occurred on the mitochondrial tRNAs. These sites may be unproductive mitoribosome binding events or simply from tRNAs partially digesting during MNase treatment. Future work is needed to understand whether these are actual translation events and to determine the function of these potential novel peptides. Together, our findings improve our understanding of mitochondrial translation initiation, gene expression, and the mechanisms of translation inhibition.

Materials and Methods

Isolation of mitoribosomes for profiling and western blotting

Mitoribosome profiling was carried out in HEK293 Flp-In T-REx cells. 15 cm plates were treated with either DMSO as a control or 100 µg/mL of protein synthesis inhibitor for 1 hour, washed with 4°C PBS, and flash frozen by floating the plate on liquid nitrogen. Cells were collected by scraping on ice with 600 µL of lysis buffer (1.5x Lysis buffer (30 mM Tris–HCl pH 7.8, 150 mM KCl, 15 mM $MgCl_2$, 1.5 mM DTT, 1.5% Triton X-100, 0.15% NP40, 1 × complete phosphatase and protease inhibitors)) and lysed by passing through a 27-G needle 10 times. Lysate was centrifuged for 10 minutes at 21,000 g at 4°C, and the supernatant was collected. 300 µL of lysate was footprinted with either digested with 1,5000 U of MNase, 10 µL of SUPERase-In, and 5 mM of $CaCl_2$ at 22°C for 1 hour and stopped by adding EGTA to a concentration of 6 mM or with 8 U/µL of RNase I at 22°C for 1 hour and stopped by adding 10 µL of SUPERase-In. Titration of the digestion enzymes was not performed and is based on previous published work[29,50]. The digestion was clarified by centrifugation at 21,000 g for 5 minutes. Lysates were loaded onto a 5%-30% sucrose gradient (20 mM Tris-HCl, pH 7.8, 100 mM KCl, 10mM $MgCl_2$, 1 mM DTT) and spun for 2.5 hours at 40,000 rpm in a SW40 rotor. 55S mitoribosome fractions were collected using a BioComp Fractionator and MRPFs were isolated by SDS/hot phenol/chloroform extraction.

Mitoribosome profiling library construction

Samples were run on a 15% TBE-Urea polyacrylamide gel and footprint sizes from 15-34 nts were excised and footprints were eluted in 0.3 M NaOAc, 1 mM EDTA, and 0.25% SDS followed by purification by Oligo Clean & Concentrator. Samples were treated with Quick CIP. 3' adapters (5'-rAppNN-6 nt UMI-TGGAATTCTCGGGTGCCAAGG-L) were ligated using Rnl2(1-249)K227Q ligase for 2 hours at 16°C and pooled. Pooled samples were treated with T4 PNK for 30 minutes at 37°C. A 5' chimeric DNA-RNA adapter (GTTCAGAGTTCTACAGTCCGACGATCrNrNrNrN) was ligated to the samples with T4 RNL1. Reverse transcription was carried out using SuperScript IV followed by PCR amplification by Taq DNA polymerase. Libraries were size selected using a 3% agarose Pippin prep and final libraries were PCR amplified. Samples were sequenced as either single- or paired-end 50 nt reads on either a NextSeq550 or NovaSeq.

Mitoribosome profiling analysis

Adapter sequences were removed with cutadapt and aligned with bowtie2 to a fasta containing rRNA and tRNA sequences. To identify stalling sites, reads were mapped to a custom mitochondrial transcriptome containing all 5' UTRs, coding sequences, and 3' UTRs for all processed mRNAs. Reads were aligned with bowtie2. A 13-nt P-site offset was assigned using Plastid and mapping reads relative to the start codons of *ND4*, *ATP6*, *MT-ND5-dORF*. We determined the relative ribosome density by normalizing the number of reads at each codon by the total number of reads mapping to its respective gene for each sample. Fold change was then calculated by dividing the relative ribosome density in a treated sample by that in an untreated sample, excluding sites that carried less than 0.1% of the total ribosome density of each gene. To identify putative novel translation initiation sites, we mapped our footprints to the entire mitochondrial genome and visually inspected the 3' ends of mitochondrial tRNAs and rRNAs.

Mass spectrometry analysis of mitochondrial proteins

Mitochondria were isolated from 2×10^7 HEK293 cells using the Mitochondria Isolation Kit for Cultured Cells (Thermo Scientific). Mitochondrial proteins were processed for trypsin/LysC digestion, and the digested peptide mixture was then concentrated and desalted using C18 column. Reconstituted desalted peptides in 25 µl of 0.1% formic acid. 12 µl of peptides from each sample was analyzed by a 110 min LC/MS/MS run. The LC/MS/MS analysis of tryptic peptides for each sample was performed sequentially with a blank run between each two sample runs using a Thermo Scientific Orbitrap Exploris 240 Mass Spectrometer and a Thermo Dionex UltiMate 3000 RSLCnano System. Peptides from trypsin digestion were loaded onto a peptide trap cartridge at a flow rate of 5 µL/min. The trapped peptides were eluted onto a reversed-phase Easy-Spray Column PepMap RSLC, C18, 2 µM, 100A, 75 µm × 250 mm (Thermo Scientific) using a linear gradient of acetonitrile (3-36%) in 0.1% formic acid. The elution duration was 60 min at a flow rate of 0.3 µl/min. Eluted peptides from the Easy-Spray column were ionized and sprayed into the mass spectrometer, using a Nano Easy-Spray Ion Source (Thermo) under the following settings: spray voltage, 1.6 kV, Capillary temperature, 275°C. Other settings were empirically determined. Raw data files were searched against the human protein sequences database and the client target protein sequences database using the Proteome Discoverer 2.5 software (Thermo, San Jose, CA) based on the SEQUEST algorithm. Carbamidomethylation (+57.021 Da) of cysteines was set as a fixed modification, and Oxidation / +15.995 Da (M), Phospho / +79.966 Da (S, T, Y), and Deamidated / +0.984 Da (N, Q) were set as dynamic modifications. The minimum peptide length was specified to be five amino acids. The precursor mass tolerance was set to 15 ppm, whereas the fragment mass tolerance was set to 0.05 Da. The maximum false peptide discovery rate was specified as 0.01. The resulting Proteome Discoverer Report contains all assembled proteins with peptides sequences and peptide spectrum match counts (PSM#) and MS1 peak area relative abundance.

Supplementary Figures and Tables

	Nucleotide 1	Nucleotide 2	Nucleotide 3
MT-ND1	0.407	0.321	0.272
MT-ND2	0.381	0.332	0.287
MT-CO1	0.406	0.297	0.297
MT-CO2	0.396	0.314	0.290
MT-ATP8	0.386	0.303	0.311
MT-ATP6	0.382	0.321	0.297
MT-CO3	0.387	0.304	0.308
MT-ND3	0.404	0.302	0.293
MT-ND4L	0.359	0.347	0.294
MT-ND4	0.418	0.302	0.280
MT-ND5	0.385	0.337	0.278
MT-ND6	0.369	0.294	0.338
MT-CYB	0.408	0.304	0.287
MT-RNR1_ORF	0.365	0.347	0.288
MT-RNR1_ncRNA	0.338	0.331	0.331
MT-Humanin	0.345	0.376	0.279
MT-TI	0.030	0.685	0.284
MT-TS1	0.245	0.460	0.296

Table S1. Read phasing values for mitoribosomes footprinted with RNaseI. The read phasing values for the canonical and putative ORFs.

Figure S1. **Mitoribosome profiling traces of *MT-CYB*.**

Individual traces from mitoribosome profiling from each untreated control labeled with its' corresponding antibiotic-treated sample.

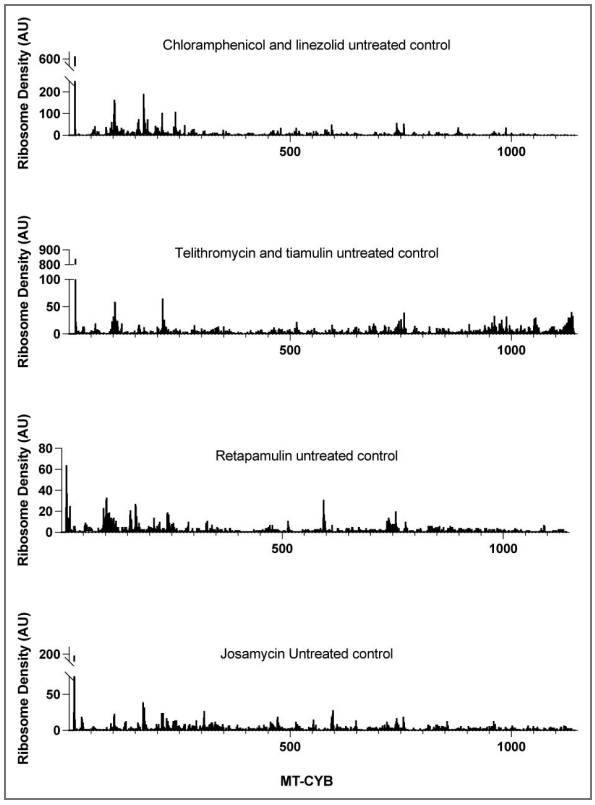

Figure S2. **Distribution of A/R/K-X-K telithromycin stalling site.**

(A) The frequency of each telithromycin stalling sites across canonical mtDNA-encoded genes and (B) the measured log fold change at those sites as compared to an untreated control.

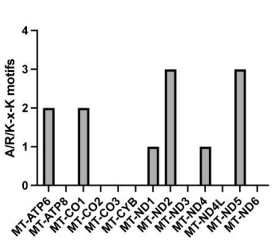

B

Gene	Stall site (codon)	Log Fold Change	Stall Motif	Length of Gene (codons)
MT-ND4	80	55.66929134	RKK	459
MT-ND2	104	34.63291139	AMK	347
MT-ATP6	96	13.34866237	KIK	226
MT-CO1	480	8.44860196	KRK	513
MT-ATP6	94	7.213050223	RSK	226
MT-ND1	53	6.980821918	AMK	318
MT-ND5	511	6.752314298	KLK	603
MT-ND2	57	4.222222222	AIK	347
MT-CO1	478	4.049649208	ASK	513
MT-ND2	313	2.738072055	KMK	347
MT-ND5	513	1.706953542	KMK	603
MT-ND5	222	0.9491412	AGK	603

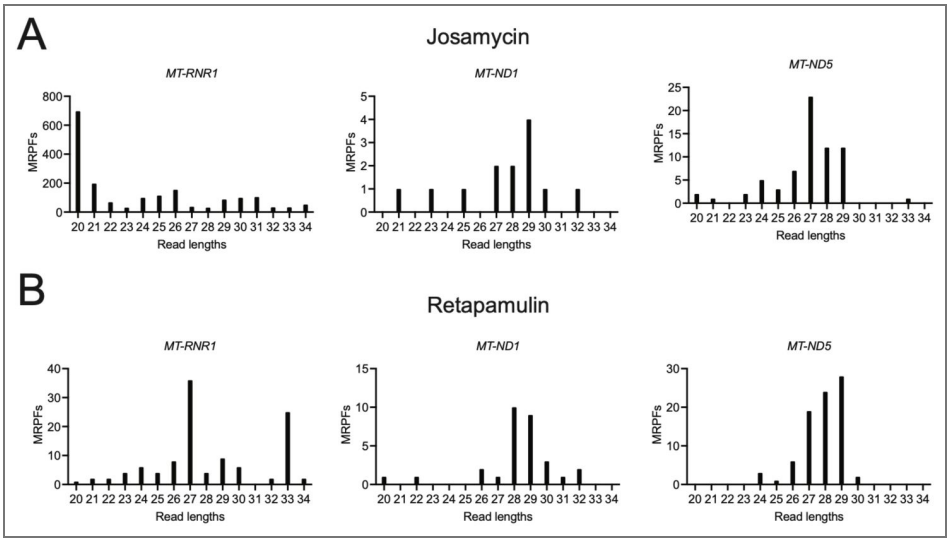

Figure S3. MRPF lengths after treatment with initiation inhibitors correlate to alternative initiation sites.

(A) Read lengths of MNase-generated MRPFs from cells treated with josamycin or (B) retapamulin.

Data availability

Mitoribosome fastq files, wig files mapping to mitochondrial mRNAs, and read length files for MNase-treated samples mapping to chrM are available through GEO Series GSE277563. All data generated or analyzed during this study are included in the manuscript and supporting files; source data files have been provided for all figures.

Acknowledgements

We'd like to thank Nicholas Guydosh (NIDDK), Sezen Meydan (Vanderbilt University), Astrid Haase (NIDDK), the Haase lab members, and the Hafner lab members for their feedback on this work. We thank Daniel Benhalvey (Tel Aviv University) for his assistance in carrying out ribosome profiling and Sarah Young-Baird (Uniformed Services University) for assistance with sucrose gradient fractionation. We thank Stefania Dell'Orso and Faiza Naz (NIH/NIAMS Genomic Technology Section) for sequencing experiments. This research was supported by the Intramural Research Program of the National Institutes of Health (NIH). The contributions of the NIH authors are considered Works of the United States Government. The findings and conclusions presented in this paper are those of the authors and do not necessarily reflect the views of the NIH or the U.S. Department of Health and Human Services.

Additional information

Author contributions

J.M. conceived the project, designed and executed experiments, analyzed data, and wrote the manuscript. E.Y. analyzed mitoribosome profiling data. M.H. supervised the project, advised on data interpretation and experimental design, and edited the manuscript.

Funding

Intramural Research Program of the National Institutes of Health, National Institute of Arthritis and Musculoskeletal and Skin Diseases (ZIA-AR041205 to M.H.).

Funding

Funder	Grant reference number	Author
HHS | NIH | National Institute of Arthritis and Musculoskeletal and Skin Diseases (NIAMS)	ZIA-AR041205	James Marks Emma A Young Markus Hafner

Author ORCID iDs

Markus Hafner: https://orcid.org/0000-0002-4336-6518

Additional files

Supplemental File 1 Peptides identified by protein mass spectrometry of isolated mitochondria.

References

1. **Gray M.W.**, Burger G., Lang B.F (1999) Mitochondrial evolution. *Science* **283**:1476-1481 https://doi.org/10.1126/science.283.5407.1476
2. **D'Souza A.R.**, Minczuk M (2018) Mitochondrial transcription and translation: overview. *Essays Biochem* **62**:309-320 https://doi.org/10.1042/EBC20170102

3. **Enriquez J.A.,** Chomyn A., Attardi G (1995) MtDNA mutation in MERRF syndrome causes defective aminoacylation of tRNA(Lys) and premature translation termination. *Nat Genet* **10**:47-55 https://doi.org/10.1038/ng0595-47
4. **Webb B.D.,** Diaz G.A., Prasun P (2020) Mitochondrial translation defects and human disease. *J Transl Genet Genom* **4**:71-80 https://doi.org/10.20517/jtgg.2020.11
5. **Prezant T.R.,** Agapian J.V., Bohlman M.C., Bu X., Oztas S., Qiu W.Q., Arnos K.S., Cortopassi G.A., Jaber L., Rotter J.I., *et al.* (1993) Mitochondrial ribosomal RNA mutation associated with both antibiotic-induced and non-syndromic deafness. *Nat Genet* **4**:289-294 https://doi.org/10.1038/ng0793-289
6. **Zheng J.,** Ji Y., Guan M.X (2012) Mitochondrial tRNA mutations associated with deafness. *Mitochondrion* **12**:406-413 https://doi.org/10.1016/j.mito.2012.04.001
7. **Smick K.M.,** Condit P.K., Proctor R.L., Sutcher V (1964) Fatal Aplastic Anemia. An Epidemiological Study of Its Relationship to the Drug Chloramphenicol. *J Chronic Dis* **17**:899-914 https://doi.org/10.1016/0021-9681(64)90161-4
8. **Woodhead J.L.,** Yang K., Oldach D., MacLauchlin C., Fernandes P., Watkins P.B., Siler S.Q., Howell B.A (2019) Analyzing the Mechanisms Behind Macrolide Antibiotic-Induced Liver Injury Using Quantitative Systems Toxicology Modeling. *Pharm Res* **36** https://doi.org/10.1007/s11095-019-2582-y
9. **De Vriese A.S.,** Coster R.V., Smet J., Seneca S., Lovering A., Van Haute L.L., Vanopdenbosch L.J., Martin J.J., Groote C.C., Vandecasteele S., *et al.* (2006) Linezolid-induced inhibition of mitochondrial protein synthesis. *Clin Infect Dis* **42**:1111-1117 https://doi.org/10.1086/501356
10. **Gupta A.,** Okesli-Armlovich A., Morgens D., Bassik M.C., Khosla C (2020) A genome-wide analysis of targets of macrolide antibiotics in mammalian cells. *J Biol Chem* **295**:2057-2067 https://doi.org/10.1074/jbc.RA119.010770
11. **Amunts A.,** Brown A., Toots J., Scheres S.H.W., Ramakrishnan V (2015) Ribosome. The structure of the human mitochondrial ribosome. *Science* **348**:95-98 https://doi.org/10.1126/science.aaa1193
12. **Fu X.,** Wan P., Li P., Wang J., Guo S., Zhang Y., An Y., Ye C., Liu Z., Gao J., *et al.* (2021) Mechanism and Prevention of Ototoxicity Induced by Aminoglycosides. *Front Cell Neurosci* **15**:692762 https://doi.org/10.3389/fncel.2021.692762
13. **Morales-Alvarez M.C** (2020) Nephrotoxicity of Antimicrobials and Antibiotics. *Adv Chronic Kidney Dis* **27**:31-37 https://doi.org/10.1053/j.ackd.2019.08.001
14. **Soriano A.,** Miro O., Mensa J (2005) Mitochondrial toxicity associated with linezolid. *N Engl J Med* **353**:2305-2306 https://doi.org/10.1056/NEJM200511243532123
15. **Palenzuela L.,** Hahn N.M., Nelson R.P., Arno J.N., Schobert C., Bethel R., Ostrowski L.A., Sharma M.R., Datta P.P., Agrawal R.K., *et al.* (2005) Does linezolid cause lactic acidosis by inhibiting mitochondrial protein synthesis?. *Clin Infect Dis* **40**:e113-116 https://doi.org/10.1086/430441
16. **Bale B.I.,** Elebesunu E.E., Manikavasagar P., Agwuna F.O., Ogunkola I.O., Sow A.U., Lucero-Prisno D.E (2023) Antibiotic resistance in ocular bacterial infections: an integrative review of ophthalmic chloramphenicol. *Trop Med Health* **51**:15 https://doi.org/10.1186/s41182-023-00496-x
17. **Lorenzo D** (2019) Chloramphenicol Resurrected: A Journey from Antibiotic Resistance in Eye Infections to Biofilm and Ocular Microbiota. *Microorganisms* **7** https://doi.org/10.3390/microorganisms7090278
18. **Browne A.J.,** Chipeta M.G., Haines-Woodhouse G., Kumaran E.P.A., Hamadani B.H.K., Zaraa S., Henry N.J., Deshpande A., Reiner R.C., Day N.P.J., *et al.* (2021) Global antibiotic consumption and usage in humans, 2000-18: a spatial modelling study. *Lancet Planet Health* **5**:e893-e904 https://doi.org/10.1016/S2542-5196(21)00280-1
19. **Graham D.J** (2006) Telithromycin and acute liver failure. *N Engl J Med* **355**:2260-2261 https://doi.org/10.1056/NEJMc066372
20. **Paternoga H.,** Crowe-McAuliffe C., Bock L.V., Koller T.O., Morici M., Beckert B., Myasnikov A.G., Grubmuller H., Novacek J., Wilson D.N (2023) Structural conservation of antibiotic interaction with ribosomes. *Nat Struct Mol Biol* **30**:1380-1392 https://doi.org/10.1038/s41594-023-01047-y

21. **Lin J.,** Zhou D., Steitz T.A., Polikanov Y.S., Gagnon M.G (2018) Ribosome-Targeting Antibiotics: Modes of Action, Mechanisms of Resistance, and Implications for Drug Design. *Annu Rev Biochem* **87**:451-478 https://doi.org/10.1146/annurev-biochem-062917-011942

22. **Yan K.,** Madden L., Choudhry A.E., Voigt C.S., Copeland R.A., Gontarek R.R (2006) Biochemical characterization of the interactions of the novel pleuromutilin derivative retapamulin with bacterial ribosomes. *Antimicrob Agents Chemother* **50**:3875-3881 https://doi.org/10.1128/AAC.00184-06

23. **Meydan S.,** Marks J., Klepacki D., Sharma V., Baranov P.V., Firth A.E., Margus T., Kefi A., Vazquez-Laslop N., Mankin A.S (2019) Retapamulin-Assisted Ribosome Profiling Reveals the Alternative Bacterial Proteome. *Mol Cell* **74**:481-493.e486. https://doi.org/10.1016/j.molcel.2019.02.017

24. **Choi J.,** Marks J., Zhang J., Chen D.H., Wang J., Vazquez-Laslop N., Mankin A.S., Puglisi J.D (2020) Dynamics of the context-specific translation arrest by chloramphenicol and linezolid. *Nat Chem Biol* **16**:310-317 https://doi.org/10.1038/s41589-019-0423-2

25. **Marks J.,** Kannan K., Roncase E.J., Klepacki D., Kefi A., Orelle C., Vazquez-Laslop N., Mankin A.S (2016) Context-specific inhibition of translation by ribosomal antibiotics targeting the peptidyl transferase center. *Proc Natl Acad Sci U S A* **113**:12150-12155 https://doi.org/10.1073/pnas.1613055113

26. **Itoh Y.,** Singh V., Khawaja A., Naschberger A., Nguyen M.D., Rorbach J., Amunts A. (2022) Structure of the mitoribosomal small subunit with streptomycin reveals Fe-S clusters and physiological molecules. *eLife* **11** https://doi.org/10.7554/eLife.77460

27. **Amunts A.,** Brown A., Bai X.C., Llacer J.L., Hussain T., Emsley P., Long F., Murshudov G., Scheres S.H.W., Ramakrishnan V (2014) Structure of the yeast mitochondrial large ribosomal subunit. *Science* **343**:1485-1489 https://doi.org/10.1126/science.1249410

28. **Li S.H.,** Nofal M., Parsons L.R., Rabinowitz J.D., Gitai Z (2021) Monitoring mammalian mitochondrial translation with MitoRiboSeq. *Nat Protoc* **16**:2802-2825 https://doi.org/10.1038/s41596-021-00517-1

29. **Rooijers K.,** Loayza-Puch F., Nijtmans L.G., Agami R (2013) Ribosome profiling reveals features of normal and disease-associated mitochondrial translation. *Nat Commun* **4** https://doi.org/10.1038/ncomms3886

30. **Sothiselvam S.,** Neuner S., Rigger L., Klepacki D., Micura R., Vazquez-Laslop N., Mankin A.S (2016) Binding of Macrolide Antibiotics Leads to Ribosomal Selection against Specific Substrates Based on Their Charge and Size. *Cell Rep* **16**:1789-1799 https://doi.org/10.1016/j.celrep.2016.07.018

31. **Schlunzen F.,** Pyetan E., Fucini P., Yonath A., Harms J.M (2004) Inhibition of peptide bond formation by pleuromutilins: the structure of the 50S ribosomal subunit from Deinococcus radiodurans in complex with tiamulin. *Mol Microbiol* **54**:1287-1294 https://doi.org/10.1111/j.1365-2958.2004.04346.x

32. **Poulsen S.M.,** Karlsson M., Johansson L.B., Vester B (2001) The pleuromutilin drugs tiamulin and valnemulin bind to the RNA at the peptidyl transferase centre on the ribosome. *Mol Microbiol* **41**:1091-1099 https://doi.org/10.1046/j.1365-2958.2001.02595.x

33. **Davidovich C.,** Bashan A., Auerbach-Nevo T., Yaggie R.D., Gontarek R.R., Yonath A (2007) Induced-fit tightens pleuromutilins binding to ribosomes and remote interactions enable their selectivity. *Proc Natl Acad Sci U S A* **104**:4291-4296 https://doi.org/10.1073/pnas.0700041104

34. **Arenz S.,** Ramu H., Gupta P., Berninghausen O., Beckmann R., Vazquez-Laslop N., Mankin A.S., Wilson D.N (2014) Molecular basis for erythromycin-dependent ribosome stalling during translation of the ErmBL leader peptide. *Nat Commun* **5** https://doi.org/10.1038/ncomms4501

35. **Beckert B.,** Leroy E.C., Sothiselvam S., Bock L.V., Svetlov M.S., Graf M., Arenz S., Abdelshahid M., Seip B., Grubmuller H., *et al.* (2021) Structural and mechanistic basis for translation inhibition by macrolide and ketolide antibiotics. *Nat Commun* **12** https://doi.org/10.1038/s41467-021-24674-9

36. **Dubot A.,** Godinot C., Dumur V., Sablonniere B., Stojkovic T., Cuisset J.M., Vojtiskova A., Pecina P., Jesina P., Houstek J (2004) GUG is an efficient initiation codon to translate the human mitochondrial ATP6 gene. *Biochem Biophys Res Commun* **313**:687-693 https://doi.org/10.1016/j.bbrc.2003.12.013

37. **Kruger A.,** Remes C., Shiriaev D.I., Liu Y., Spahr H., Wibom R., Atanassov I., Nguyen M.D., Cooperman B.S., Rorbach J (2023) Human mitochondria require mtRF1 for translation termination at non-canonical stop codons. *Nat Commun* **14** https://doi.org/10.1038/s41467-022-35684-6

38. **Tsai K.,** Stojkovic V., Lee D.J., Young I.D., Szal T., Klepacki D., Vazquez-Laslop N., Mankin A.S., Fraser J.S., Fujimori D.G (2022) Structural basis for context-specific inhibition of translation by oxazolidinone antibiotics. *Nat Struct Mol Biol* **29**:162-171 https://doi.org/10.1038/s41594-022-00723-9

39. **Syroegin E.A.,** Flemmich L., Klepacki D., Vazquez-Laslop N., Micura R., Polikanov Y.S (2022) Structural basis for the context-specific action of the classic peptidyl transferase inhibitor chloramphenicol. *Nat Struct Mol Biol* **29**:152-161 https://doi.org/10.1038/s41594-022-00720-y

40. **Wakigawa T.,** Mito M., Yamashiro H., Tomuro K., Tani H., Tomizawa K., Chujo T., Nagao A., Suzuki T., Wei F.-Y., *et al.* (2023) Complexity and dynamics of *in organello* translation landscape assessed by high-resolution mitochondrial ribosome profiling. *bioRxiv* https://doi.org/10.1101/2023.07.19.549812

41. **Bibel B.,** Raskar T., Couvillion M., Lee M., Kleinman J.I., Takeuchi-Tomita N., Churchman L.S., Fraser J.S., Fujimori D.G. (2024) Context-specific inhibition of mitochondrial ribosomes by phenicol and oxazolidinone antibiotics. *bioRxiv* https://doi.org/10.1101/2024.08.21.609012

42. **Brandon M.C.,** Lott M.T., Nguyen K.C., Spolim S., Navathe S.B., Baldi P., Wallace D.C (2005) MITOMAP: a human mitochondrial genome database--2004 update. *Nucleic Acids Res* **33**:D611-613 https://doi.org/10.1093/nar/gki079

43. **Kalghatgi S.,** Spina C.S., Costello J.C., Liesa M., Morones-Ramirez J.R., Slomovic S., Molina A., Shirihai O.S., Collins J.J. (2013) Bactericidal antibiotics induce mitochondrial dysfunction and oxidative damage in Mammalian cells. *Sci Transl Med* **5**:192ra185 https://doi.org/10.1126/scitranslmed.3006055

44. **D'Achille G.,** Morroni G (2023) Side effects of antibiotics and perturbations of mitochondria functions. *Int Rev Cell Mol Biol* **377**:121-139 https://doi.org/10.1016/bs.ircmb.2023.03.009

45. **Desai N.,** Yang H., Chandrasekaran V., Kazi R., Minczuk M., Ramakrishnan V (2020) Elongational stalling activates mitoribosome-associated quality control. *Science* **370**:1105-1110 https://doi.org/10.1126/science.abc7782

46. **Singh V.,** Itoh Y., Del'Olio S., Hassan A., Naschberger A., Flygaard R.K., Nobe Y., Izumikawa K., Aibara S., Andrell J., *et al.* (2024) Mitoribosome structure with cofactors and modifications reveals mechanism of ligand binding and interactions with L1 stalk. *Nat Commun* **15** https://doi.org/10.1038/s41467-024-48163-x

47. **Kong Q.P.,** Yao Y.G., Sun C., Zhu C.L., Zhong L., Wang C.Y., Cai W.W., Xu X.M., Xu A.L., Zhang Y.P (2004) Phylogeographic analysis of mitochondrial DNA haplogroup F2 in China reveals T12338C in the initiation codon of the ND5 gene not to be pathogenic. *J Hum Genet* **49**:414-423 https://doi.org/10.1007/s10038-004-0170-3

48. **Vilarinho L.,** Chorao R., Cardoso M.L., Rocha H., Nogueira C., Santorelli F.M (1999) The ND1 T3308C mutation may be a mtDNA polymorphism. Report of two Portuguese patients. *J Inherit Metab Dis* **22**:90-91 https://doi.org/10.1023/a:1005471904710

49. **Rocha H.,** Flores C., Campos Y., Arenas J., Vilarinho L., Santorelli F.M., Torroni A. (1999) About the "Pathological" role of the mtDNA T3308C mutationellipsis. *Am J Hum Genet* **65**:1457-1459 https://doi.org/10.1086/302641

50. **Soto I.,** Couvillion M., Hansen K.G., McShane E., Moran J.C., Barrientos A., Churchman L.S (2022) Balanced mitochondrial and cytosolic translatomes underlie the biogenesis of human respiratory complexes. *Genome Biol* **23** https://doi.org/10.1186/s13059-022-02732-9

51. **Fiedler M.,** Rossmanith W., Wahle E., Rammelt C (2015) Mitochondrial poly(A) polymerase is involved in tRNA repair. *Nucleic Acids Res* **43**:9937-9949 https://doi.org/10.1093/nar/gkv891

Peer reviews

Reviewer #1 (Public review):

Summary:

This study aimed to determine whether bacterial translation inhibitors affect mitochondria through the same mechanisms. Using mitoribosome profiling, the authors found that most antibiotics, except telithromycin, act similarly in both systems. These insights could help in the development of antibiotics with reduced mitochondrial toxicity.

They also identified potential novel mitochondrial translation events, proposing new initiation sites for *MT-ND1* and *MT-ND5*. These insights not only challenge existing annotations but also open new avenues for research on mitochondrial function.

Strengths:

Ribosome profiling is a state-of-the-art method for monitoring the translatome at very high resolution. Using mitoribosome profiling, the authors convincingly demonstrate that most of the analyzed antibiotics act in the same way on both bacterial and mitochondrial ribosomes, except for telithromycin. Additionally, the authors report possible alternative translation events, raising new questions about the mechanisms behind mitochondrial initiation and start codon recognition in mammals.

Weaknesses:

All the weaknesses I previously highlighted were adequately addressed.

https://doi.org/10.7554/eLife.103699.2.sa2

Reviewer #3 (Public review):

Summary:

Recently, the off-target activity of antibiotics on human mitoribosome has been paid more attention in the mitochondrial field. Hafner et al applied mitoribosome profilling to study the effect of antibiotics on protein translation in mitochondria as there are similarities between bacterial ribosome and mitoribosome. The authors conclude that some antibiotics act on mitochondrial translation initiation by the same mechanism as in bacteria. On the other hand, the authors showed that chloramphenicol, linezolid and telithromycin trap mitochondrial translation in a context-dependent manner. More interesting, during deep analysis of 5' end of ORF, the authors reported the alternative start codon for ND1 and ND5 proteins instead of previously known one. This is a novel finding in the field and it also provide another application of the technique to further study on mitochondrial translation.

Strengths:

This is the first study which applied mitoribosome profiling method to analyze mutiple antibiotics treatment cells. The mitoribosome profiling method had been optimized carefully and has been suggested to be a novel method to study translation events in mitochondria. The manuscript is constructive and well-written.

Weaknesses:

This is a novel and interesting study, however, most of conclusion comes from mitoribosome profiling analysis, as the result, the manuscript lacks the cellular biochemical data to provide more evidence and support the findings.

Comments on revisions:

The authors addressed most of my concerns and comments, although there is still no biochemical assay which should be performed to support mitoribsome profiling data.

The author also carefully investigated the structure of complex I, however, I am surprised that the author chose to analyse a low resolution structure (3.7 A). Recently, there are more high resolution structures of mammalian complex I published (7R41, 7V2C, 7QSM, 9I4I). Furthermore, the authors should not only respond to the reviewers but also (somehow) discuss these points in the manuscript.

https://doi.org/10.7554/eLife.103699.2.sa1

Author response:

The following is the authors' response to the original reviews.

> ***Public Reviews:***
>
> ***Reviewer #1 (Public review):***
>
> *Summary:*
>
> *This study aimed to determine whether bacterial translation inhibitors affect mitochondria through the same mechanisms. Using mitoribosome profiling, the authors found that most antibiotics, except telithromycin, act similarly in both systems. These insights could help in the development of antibiotics with reduced mitochondrial toxicity.*
>
> *They also identified potential novel mitochondrial translation events, proposing new initiation sites for MT-ND1 and MT-ND5. These insights not only challenge existing annotations but also open new avenues for research on mitochondrial function.*
>
> *Strengths:*
>
> *Ribosome profiling is a state-of-the-art method for monitoring the translatome at very high resolution. Using mitoribosome profiling, the authors convincingly demonstrate that most of the analyzed antibiotics act in the same way on both bacterial and mitochondrial ribosomes, except for telithromycin. Additionally, the authors report possible alternative translation events, raising new questions about the mechanisms behind mitochondrial initiation and start codon recognition in mammals.*
>
> *Weaknesses:*
>
> *The main weaknesses of this study are:*
>
> *While the authors highlight an interesting difference in the inhibitory mechanism of telithromycin on bacterial and mitochondrial ribosomes, mechanistic explanations or hypotheses are lacking.*

We acknowledge that we were not able to present a clear explanation for potential mechanistic differences of telithromycin inhibition between mitochondrial and bacterial ribosomes. In future work, structural analyses in collaboration with experts will provide these insights.

> *The assignment of alternative start codons in MT-ND1 and MT-ND5 is very interesting but does not seem to fully align with structural data.*

We appreciate the reviewer's comment and consulted a cryo-EM expert to review our findings in the context of the available structural data. We downloaded the density map and reviewed the N-termini of *MT-ND1* and *MT-ND5*. We only observed the density of the N-terminus of *MT-ND1* at low confidence. At an RMSD of 2, we could not observe density for the side chains of Met and Pro, and there are gaps in the density for what is modeled as the main chain. The assignment of these residues may have been overlooked due to the expectation that they should be present in the peptide.

For *MT-ND5*, we did observe some density that could be part of the main chain; however, it did not fill out until we reduced the stringency, and we did not observe density mapping to side chain residues. To summarize, we do not confidently see density for either the side chain or the main chain for either peptide.

> *The newly proposed translation events in the ncRNAs are preliminary and should be further substantiated with additional evidence or interpreted with more caution.*

We agree with the reviewer that we did not provide conclusive evidence that our phased ribosome footprinting data on mitochondrial non-coding RNAs are proof of novel translation events. We do acknowledge this in the main text:" Due to both the short ORFs, minimal read coverage, and lack of a detectable peptide we could not determine if translation elongation occurred on the mitochondrial tRNAs. These sites may be unproductive mitoribosome binding events or simply from tRNAs partially digesting during MNase treatment."

> ***Reviewer #2 (Public review):***
>
> *In this study, the authors set out to explore how antibiotics known to inhibit bacterial protein synthesis also affect mitoribosomes in HEK cells. They achieved this through mitoribosome profiling, where RNase I and Mnase were used to generate mitoribosome-protected fragments, followed by sequencing to map the regions where translation arrest occurs. This profiling identified the codon-specific impact of antibiotics on mitochondrial translation.*
>
> *The study finds that most antibiotics tested inhibit mitochondrial translation similarly to their bacterial counterparts, except telithromycin, which exhibited distinct stalling patterns. Specifically, chloramphenicol and linezolid selectively inhibited translation when certain amino acids were in the penultimate position of the nascent peptide, which aligns with their known bacterial mechanism. Telithromycin stalls translation at an R/K-X-R/K motif in bacteria, and the study demonstrated a preference for arresting at an R/K/A-X-K motif in mitochondria. Additionally, alternative translation initiation sites were identified in MT-ND1 and MT-ND5, with non-canonical start codons. Overall, the paper presents a comprehensive analysis of antibiotics in the context of mitochondrial translation toxicity, and the identification of alternative translation initiation sites will provide valuable insights for researchers in the mitochondrial translation field.*
>
> *From my perspective as a structural biologist working on the human mitoribosome, I appreciate the use of mitoribosome profiling to explore off-target antibiotic effects and the discovery of alternative mitochondrial translation initiation sites. However, the description is somewhat limited by a focus on this single methodology. The authors could strengthen their discussion by incorporating structural approaches, which have contributed significantly to the field. For example, antibiotics such as paromomycin and linezolid have been modeled in the human mitoribosome (PMID: 25838379), while streptomycin has been resolved (10.7554/eLife.77460), and erythromycin was previously discussed (PMID: 24675956). The reason we can now describe off-target effects more meaningfully is due to the availability of fully modified human mitoribosome structures, including mitochondria-specific modifications and their roles in stabilizing the decoding center and binding ligands, mRNA, and tRNAs (10.1038/s41467-024-48163-x).*

> *These and other relevant studies should be acknowledged throughout the paper to provide additional context.*

We appreciate the work that has previously revealed how different antibiotics bind the mitochondrial ribosome. We have included these references in the manuscript to provide background and context for this work in relationship to the field.

> ***Reviewer #3 (Public review):***
>
> *Summary:*
>
> *Recently, the off-target activity of antibiotics on human mitoribosome has been paid more attention in the mitochondrial field. Hafner et al applied mitoribosome profilling to study the effect of antibiotics on protein translation in mitochondria as there are similarities between bacterial ribosome and mitoribosome. The authors conclude that some antibiotics act on mitochondrial translation initiation by the same mechanism as in bacteria. On the other hand, the authors showed that chloramphenicol, linezolid and telithromycin trap mitochondrial translation in a context-dependent manner. More interesting, during deep analysis of 5' end of ORF, the authors reported the alternative start codon for ND1 and ND5 proteins instead of previously known one. This is a novel finding in the field and it also provides another application of the technique to further study on mitochondrial translation.*
>
> *Strengths:*
>
> *This is the first study which applied mitoribosome profiling method to analyze mutiple antibiotics treatment cells.*
>
> *The mitoribosome profiling method had been optimized carefully and has been suggested to be a novel method to study translation events in mitochondria. The manuscript is constructive and written well.*
>
> *Weaknesses:*
>
> *This is a novel and interesting study, however, most of the conclusion comes from mitoribosome profiling analysis, as a result, the manuscript lacks the cellular biochemical data to provide more evidence and support the findings.*

We thank the reviewer for the positive assessment of our work. We agree that future biochemical and structural experiments will strengthen the conclusions we derive from the ribosome profiling.

> ***Recommendations for the authors:***
>
> ***Reviewer #1 (Recommendations for the authors):***
>
> *In Fig. 1A, the quality of the Western blot for the sucrose gradient is suboptimal. I recommend enhancing the quality of the Western blot image and providing the sucrose gradient sedimentation patterns for both the mtSSU and mtLSU to confirm the accurate selection of the monosome fraction. Additionally, to correctly assign the A260 peaks to mitochondrial and cytosolic ribosomes, it would be helpful to include markers for both the cytoribosomal LSU and SSU, too. Furthermore, do the authors observe mitochondrial polysomes in their sucrose gradient? If so, were those fractions fully excluded from the analysis?*

We repeated our sucrose gradient and Western blotting with antibodies for the large and small subunits of the mitoribosome. We did not repeat western blotting for the cytoribosomes as the 40S, 60S, and 80S peaks are present in their canonical heights and locations on a

sucrose gradient. Western blotting indicates that the large and small subunits of the mitoribosome are located in the fraction taken for mitoribo-seq. We do see trace amounts of mitoribosome in fractions past the 55S site. Those fractions were excluded from library preparation.

> *The MNase footprints exhibited a bimodal distribution, which the authors suggest may indicate that "MNase-treatment may have captured two distinct conformations of the ribosome." It would be relevant to clarify whether an enzyme titration was performed, as excessive MNase could lead to ribosomal RNA degradation, potentially influencing the footprints.*

We did not perform a titration and instead based our concentration on the protocol from Rooijers et al, 2013. We included a statement of this and a reference to the concentration in the methods.

> *Is there an explanation for why RNase I footprinting reveals a very high peak at the 5'-end of the MT-CYB transcript, whereas this is not observed with MNase footprinting?*

It is not clear. The intensity of peaks at the 5' end of the transcripts varies. We do observe that the relative intensity of the 5' peak is greater for RNase I footprinted samples than MNase-treated samples.

> *I understand that throughout the manuscript, the authors use MT-CYB as an example to illustrate the effects of the antibiotics on mitochondrial translation. However, to strengthen the generality of the conclusions, it would be beneficial to provide the read distribution across the entire mitochondrial transcriptome, possibly in the supplementary material. Additionally, I suggest including the read distribution for MT-CYB in untreated cells to improve data interpretation and enhance the clarity of figures (e.g., Figs. 1B, 2B, 3B).*

As these experiments were generated across multiple mitoribo-seq experiments, each was done with its own control experiment. It would be inaccurate to show a single trace as representative of all experiments. Instead, we include Supplementary Figure 1, which shows the untreated *MT-CYB* trace for all control samples and indicates which treatment they pair with.

> *It would be very valuable to label each individual data point in the read phasing shown in Fig. 1D with the corresponding transcripts. For improved data visualization, I suggest assigning distinct colors to each transcript.*

We are concerned that including the name of each gene in the main figure would be too difficult for the reader to accurately interpret. Instead, we have added a Supplementary Table with those values.

> *How do the authors explain the significant peak (approx. 10,000 reads) at the 5' end of the transcript in the presence of tiamulin (Fig. 2B)? Does this peak correspond to the start codon, and how does it relate to the quantification reported in Fig. 2C?*

Yes, this represents the start codon. These reads are likely derived from the start codon as they are mapping to the 5' end of the transcript. There are differences in sequencing depth depending on the experiment, so what is critical is the relative distribution of reads on the transcript rather than comparing absolute reads between experiments. *MT-CYB* has 54% of the reads at the start site, which is representative of what we see across all genes.

> *Throughout the manuscript, I found the usage of the terms "5' end" and "start codon" somewhat confusing, as they appear to be used synonymously in some instances. For example, in Fig. 2C, the y-axis label states "ribosomes at start codon," while the figure*

> *caption mentions "...percentage of reads that map to the 5' end of mitochondrial transcripts." Given the size of the graphs, it is also challenging for the reader to determine whether the peaks correspond specifically to the start codon or if multiple peaks accumulate at the initial codons.*

We were selected for this language because two different types of analysis are being carried out. Ribosome profiling carried out in Figures 2 and 3 is carried out with RNase I, which poorly maps the ribosomes at the start codon when we do the read length analysis in Figure 4. Ribosome footprint at the 5' end may include ribosomes that are on the 2-4 codons following the start codon, so it would not be accurate to label those as "ribosomes at a start codon." We have renamed the axis to "Ribosomes at 5' end". Wig files are available online for all mitoribosome profiling experiments. In this case, the assigned "P-site" is several codons after the start codon due to the offset applied and the minimal 5' UTR. Thus, it is less important to see which codon density is assigned to, but rather the general distribution of the reads.

> *The authors state, "Cells treated with telithromycin did show a slight increase in MRPF abundance at the 5' end of MT-CYB" and "the cumulative distribution of MRPFs suggested that ribosome density was biased towards the 5' end of the gene for chloramphenicol and telithromycin, but not significantly for linezolid." Could this observation be linked to the presence of specific stalling motifs in that region? If so, it would be beneficial to display such motifs on the graphs of the read distribution across the transcriptome to substantiate the context-dependent inhibition.*

Thank you for this suggestion. For chloramphenicol and linezolid, alanine, serine, and threonine make up nearly 25% of the mitochondrial proteome. As such, there are numerous stall sites across the transcript. Given their identical stalling motifs, the difference between chloramphenicol and linezolid is due to sequence-specific differences. Potentially, this could be due to conditions such as the final concentration of antibiotic inside the mitochondria and the on/off rate of an inhibitor with the translating mitoribosome. Both may affect the kinetics of stalling and allow mitoribosomes to evade early stall sites.

We have also included the sites of all A/K/R-X-K motifs located in the genome and the calculated fold change for each position. As a note, this includes sites that do not pass the minimum filter set by our analysis and we note this in the text.

The comment raises an additional question: Does the increased density at the 5' end derive from stalled mitoribosomes or queued mitoribosomes behind a stalling event? Recent work by Iwasaki's group shows that mitoribosomes can form disomes and queue behind each other. However, we could not observe 30 aa periodicities behind stalling events that would be indicative of collided mitoribosomes.

> *In Fig. 3E, the authors report an additional and very interesting observation that is not discussed. Linezolid treatment causes reduced ribosome occupancy when proline or glycine codons occupy the P-site, or when the amino acids have been incorporated into the polypeptide chain and occupy the -1 position. It is known that the translation of proline and glycine frequently leads to ribosome stalling due to the physicochemical properties of these amino acids. Has this effect of linezolid been reported in the bacterial translation system? Additionally, can the authors propose hypotheses for the mechanism behind this observation? A similar observation is noted for telithromycin when glycine occupies the same positions, as well as when aspartate occupies the P- and A-sites.*

In bacteria, Linezolid does have an "anti-stalling" motif when glycine is present in the A-site. However, this is due to the size of the residue being compatible with antibiotic binding.

The most likely cause of this effect is a redistribution of ribosome footprints. As the antibiotics introduce new arrest sites, ribosome density at other sites relatively decreases.

This is likely an artifact from mitoribosomes redistributing from endogenously slow codons to new arrest sites. When looking at carrying out our disome profiling in the presence of anisomycin, we see a similar effect. Cytoribosomes are redistributed from endogenous stalling sites, such as proline, and are redistributed throughout the gene. As a result, translation at proline appears “more efficient” upon treatment with an inhibitor but is instead an artifact of analysis.

> *Figure 3F could benefit from indicating which mtDNA-encoded protein corresponds to each of the strongest stalling motifs.*

We have included a supplementary figure to highlight which mitochondrially-encoded genes containing the R/K/A-X-K motif and noted in the text that mitochondrial translation may be unevenly inhibited.

> *The legend "increasing mRPF abundance" in Fig. 4C may be missing the corresponding colors.*

The legend applies to all sections of the figure. We double-checked the range of the colors in the tables, and they do match the legend.

> *The observation that the start codons in MT-ND1 and MT-ND5 might differ from the annotated canonical ones is intriguing. While the ribosome profiling data appear clear, mass spectrometry (MS) analysis may be misleading. The absence of evidence does not necessarily imply evidence of absence. How does this proposed conclusion correlate with the structural data obtained from HEK cells? For instance, the cryo-EM structural model of a complex I-containing human supercomplex (PDB: 5XTD, PMID: 28844695) shows the presence of Pro2 in MT-ND1 and the full-length MT-ND5 protein. The authors should carefully examine structural data to ascertain whether alternative forms of MT-ND1 and MT-ND5 are actually observed in the assembled complex I.*

We really appreciate this comment. We sat down with an expert in cryo-EM and reviewed the figure. We downloaded the density map and reviewed the N-termini of *MT-ND1* and *MT-ND5*. We only observed the density of the N-terminus of *MT-ND1* at low confidence. At an RMSD of 2, we could not observe density for the side chains of Met and Pro, and there are gaps in the density for what is modeled as the main chain. The assignment of these residues may have been overlooked due to the expectation that they should be present in the peptide.

For *MT-ND5*, we did observe some density that could be part of the main chain; however, it did not fill out until we reduced the stringency, and we did not observe density mapping to side chain residues. To summarize, we do not confidently see density for either the side chain or the main chain for either peptide.

> *Given that ribosome profiling is based on the assumption that ribosomes protect mRNA fragments from RNase digestion, interpreting the data related to Fig. 5 and the proposed existence of translation events involving ncRNAs is challenging. Most importantly, tRNAs and rRNAs are highly folded RNA molecules and, by definition, are protected by ribosomal proteins. Simultaneously, as the authors point out, "These reads could either be products of random digestion of the abundant background of ncRNAs or be genuine MRPFs." RNase I preferentially digests single-stranded RNA (ssRNA), but excess enzyme can still lead to degradation. Consequently, many random tRNA/rRNA fragments may be generated by RNase digestion, potentially resulting in artifacts. I suggest that the authors examine what happens to these reads when mitochondrial translation is inhibited.*

We have low-quality mitoribo-seq with initiation inhibitors and Mnase showing footprints of the same size. We do not have a small-molecule inhibitor that is able to completely ablate translation, as they instead stabilize mitoribosomes at different steps in translation. We have

considered alternative ways of capturing a background rRNA and tRNA digestion pattern; however, these have their own drawbacks. Dissociation with EDTA prior to digestion or carrying out library prep on the small and large subunits may capture mitoribosomes no longer in the process of translation; however, dissociated subunits would have different surfaces now available for digestion and may not capture tRNAs.

> *Regarding the statement, "While the ORF on MT-TS1 is longer, MRPF density was low and we did not observe read phasing and thus it is likely not translated (not shown)," the data should not be excluded unless a clear explanation is provided for why translation would not occur from this specific RNA.*

We have included this value in the graph as well as in Supplementary Figure 1.

> *The graph in Fig. 5B shows the periodicity of only the putative RNR1 ORF, but not that of the other proposed ORFs. What is the reason for this?*

We have included the MT-TS1 putative ORF in Figure 5 and Figure S1. Other ORFs did not have density in the ORF. If these are real mitoribosome footprints at these start codons, it may be due to them being transient binding events that never result in elongation. Alternatively, they may be due to tRNA degradation during library preparation.

> *The assumption that the UUG codon can serve as a start site for mitochondrial translation has not been substantiated. Recent data have identified translation initiation events from non-ATG/ATA codons (near-cognate and sub-cognate) using retapamulin, but UUG was not among them. Can the authors detect such events in their ribosome profiling data collected in the presence of retapamulin, tiamulin, or josamycin?*

The report of translation initiation at non-ATG/ATA codons strongly disagrees with our findings. We report that sites of translation initiation observed within annotated coding regions in mitochondria occur at the annotated start sites, while the other report finds frequent alternative initiation events. We have looked for those arrest sites and did not observe them.

> *In the section "Mitoribosome profiling reveals novel translation events," the title may be misleading given the preliminary nature of the results. To support such a claim, the authors should provide experimental evidence demonstrating that the proposed translation events genuinely exist and result in the synthesis of previously unidentified polypeptides. Alternatively, the interpretation should be approached with greater caution and more clearly indicated as preliminary.*

We agree with the reviewers that a distinction should be made between reporting truly novel translation events, like the recently reported *MT-ND5-dORF*, and sites we suspect mitoribosomes may be binding and that require detailed follow-up. We altered the section title to suggest that this may be showing novel translation events. Additionally, we included a statement in the discussion that these MRPFs may be simply tRNA digestion by RNase I.

> *Although located at the 5' end of RNR1, the newly identified ORF is situated 79 nt downstream. According to current knowledge, this appears to be a lengthened 5' UTR that may hinder mitoribosome loading. The authors should speculate on potential initiation mechanisms.*

The start of the putative ORF is not located 79 nts down, but at the 8th nucleotide. The reviewer may be including the tRNA-Phe in their calculation, which is cleaved from MT-RNR1. This start site is closer to the 5’ end than our findings with *MT-ND5*.

> *To enhance the interpretation of the mitoribosome profiling data, the authors could complement their findings with classical metabolic labeling using (35)S-methionine. This*

> *approach would allow for a different assessment of the stringency of the inhibition under the tested experimental conditions.*

We are currently working on these experiments using mito-funcats. A future direction we are taking this work is to understand how the cell responds to different mechanisms of translation inhibition. For example, we are trying to understand if telithromycin, which appears highly selective, only partially inhibits translation of the mtDNA-encoded proteome.

> ***Reviewer #2 (Recommendations for the authors):***
>
> *Other small editorial comments:*
>
> *Line 24: "translate proteins"?*

Revised for clarity

> *Line 24: The sentence describing mitochondrial translation as "closely resembling the one in prokaryotes" could be reformulated. While the core of the mitoribosome is conserved, the entire apparatus has many mitochondria-specific features.*

Since this is the abstract, we simplified the point by saying that mitoribosomes are more similar to prokaryotic than cytosolic ribosomes.

Clarified to highlight that the mitochondrial system is more similar to the bacterial system than the eukaryotic system.

> *Line 33: "novel" or "previously unrecognized" ?*

Rewritten for clarity.

> *Lines 33-35: The claim made here is not shown in the paper.*

We removed the more aspirational goal of this paper and focused on the main findings of the paper.

> *Lines 44, 47, 89 (and elsewhere): "cytoplasmic" or "cytosolic" ?*

Both terms are used in the literature. We opted for cytoplasmic as it can also include ribosomes not free in the cytosol, such as those bound to the ER.

> ***Reviewer #3 (Recommendations for the authors):***
>
> *(1) The authors should state why they chose these antibiotics for mitoribosome profiling analysis over other antibiotics from same group. Did they screen multiple antibiotics to determine the candidates for next step?*

We selected antibiotics that had a known stalling motif in bacteria (initiation or context-dependent elongation inhibitors). In addition, we carried out mitoribosome profiling with erythromycin, azithromycin, thiostrepton, and kanamycin in this work. However, we did not see any effect from these drugs in mitoribosome profiling. We are currently testing other inhibitors, such as doxycycline and tigecycline, and looking at optimizing treatment conditions to identify stalling motifs in samples that previously showed no difference.

> *(2) What is the reason for choosing the concentration of antibiotics retapamulin, tiamulin and josamycin, this is IC50 value or above this value? On the other hand, none of this information has been provided for the antibiotics in the next part. The authors should provide biochemical study for the effect of these antibiotics on cell survival and/or protein translation such as S35 assay or steady state level of mtDNA-encoded proteins upon cell treatment with these antibiotics.*

Prior to mitoribo-seq, we carried out time and concentration assays with all antibiotics. 100 µg/ml and a 30-minute treatment was tolerable for all antibiotics except retapamulin. We aimed to treat cells with a relatively high concentration of inhibitor in order to capture actively translating mitoribosomes. We were concerned that longer treatments may lead to decreased translation initiation, leading to the capture of fewer mitoribosomes. These concentrations were nearly identical to contemporary conditions carried out in Bibel et al, RNA 2025.

> *(3) Why did the authors choose MT-CYB as the representative for further analysis in the second and third parts of the manuscript?*

We chose *MT-CYB* because its length allowed for easy visualization. Some mitochondrial genes, such as *MT-ND6*, had a propensity for stronger stalling at initiation. While coverage was throughout the genes, it was difficult to visualize the changes within the ORF. Also, *MT-CYB* was less visually complex than polycistronic transcripts. All wigs were uploaded to GEO.

> *(4) Page 11, line 233-234: the authors state that telithromycin induces stalling at R/K/A-X-K motif. The authors should do further analysis on mitochondrial genome which proteins contain this motif. Furthermore, same as comment 2: the authors should confirm by 35S assay or WB to know which mtDNA-encoded proteins are affected.*

We have included a supplementary figure showing which mitochondrial genes contain these motifs.

> *(5) The results and conclusion from the fourth paragraph are very interesting. The authors suggest alternative start codon for two mtDNA encoded proteins: ND1 and ND5 based on ribosome profiling analysis. Again, I have several comments on this part:*
>
> *(a) For the accumulation of the alternative start codon of ND1 and ND5 as suggested in the manuscript, do the authors observe this trend with the initiation inhibitors used in the second paragraphs of the manuscript?*

We did not observe similar read lengths with retapamulin, tiamulin, or josamycin, which produced read lengths that were consistent with other RNase I footprinted samples.

> *(b) This observation was further confirmed by MS with a peptide form ND1 protein, the authors should show MS peak indicating MW of the peptide and MS/MS data for the peptide which supports this hypothesis.*

We are including the MS/MS report for this peptide.

> *(c) Interestingly, several high-resolution structures of mammalian complex I have been reported so far (PMID: 7614227, 10396290, 38870289), ND1 and ND5 protein express full sequences with fMet at the distal N-terminal. This is different to the suggestion from the manuscript. Could the author discuss or comment on that?*

This point was brought up by another reviewer. We have carefully analyzed the density map of PMID: 28844695. We sat down with an expert in cryo-EM and reviewed the figure. We downloaded the density map and reviewed the N-termini of *MT-ND1* and *MT-ND5*. We only observed the density of the N-terminus of *MT-ND1* at low confidence. At an RMSD of 2, we could not observe density for the sidechains of Met and Pro, and there is a gap in density for what is modeled as the main chain. The assignment of these residues may have been overlooked due to the expectation that they should be present in the peptide.

For *MT-ND5*, we did observe some density that could be part of the main chain; however, it did not fill out until we reduced the stringency, and we did not observe density mapping to

side chain residues. To summarize, we do not confidently see density for either the side chain or the main chain for either peptide.

> *Minor comments:*
>
> *The method should be written more accurately for easily repeating experiments by other groups. For example:*
>
> *(1) The authors should indicate what was exact HEK293 cell line used in this study.*

We have indicated the exact cell line.

> *(2) Page 22, line 471: which (number) fractions had been collected. The Western Blot analysis shown in Figure 1A should be repeated with both proteins from small and large subunits.*

We have repeated the Western blot with antibodies for large and small subunits. We took fractions 8 and 9, which are now indicated in the text and figure.

> *(3) Page 23, line 502: is this number of cells used for MS experiment is correct? Or is this number of cells per mL?*

This is correct and is based on the kit protocol. It is not cells per mL. We have clarified the kit being used in the methods.

https://doi.org/10.7554/eLife.103699.2.sa0